

Fall 2022

# Development of Novel Pyridazine Derivatives and Drug Delivery Systems Against Dengue

Janae A. Culmer

Follow this and additional works at: <https://digitalcommons.georgiasouthern.edu/etd>

 Part of the [Biochemistry Commons](#), [Cell Biology Commons](#), and the [Research Methods in Life Sciences Commons](#)

---

## Recommended Citation

Culmer, Janae A., "Development of Novel Pyridazine Derivatives and Drug Delivery Systems Against Dengue" (2022). *Electronic Theses and Dissertations*. 2501.  
<https://digitalcommons.georgiasouthern.edu/etd/2501>

This thesis (open access) is brought to you for free and open access by the Jack N. Averitt College of Graduate Studies at Digital Commons@Georgia Southern. It has been accepted for inclusion in Electronic Theses and Dissertations by an authorized administrator of Digital Commons@Georgia Southern. For more information, please contact [digitalcommons@georgiasouthern.edu](mailto:digitalcommons@georgiasouthern.edu).

# DEVELOPMENT OF NOVEL PYRIDAZINE DERIVATIVES AND DRUG DELIVERY SYSTEMS AGAINST DENGUE

by

JANAE CULMER

(Under the Direction of James Carter)

## ABSTRACT

The lack of approved vaccines, medications and treatment regimens has significantly contributed to the rapid spread of mosquito-borne viruses such as Dengue and Zika virus. The complex immunopathology of these viruses presents limitations for the development and implementation of a definitive, safe and effective approach to combat infections. Previous research has demonstrated that vector control strategies such as the elimination of larval habitats, larviciding with insecticides, the use of biological agents and the application of adulticides have been unsuccessful in the reduction of viral transmission leading to the need for the continued development of antivirals. This research proposes an approach for a drug delivery system that involves novel antivirals that suppress dengue virus in an intracellular pH specific manner with the use of micellar nanoparticles. Drug-loaded nanoparticle that dissociates when exposed to a pH of 6.0, will release drug at the targeted location in the cell, in particular, the proximal trans-Golgi network in the cell. Three (3) novel pyridazine derivatives were analyzed and possessed anti-viral activity against Zika virus through the use of cell-culture based suppression techniques. The derivatives described in this thesis will be designed and analyzed for its future potential in drug encapsulation into newly synthesized mPEG-PLA comprised micellar nanoparticles.

INDEX WORDS: Dengue, Zika, Antivirals, Micellar Nanoparticles, Drug Delivery Systems, Novel Pyridazine Derivatives, Cell Culture Based Suppression

DEVELOPMENT OF NOVEL PYRIDAZINE DERIVATIVES AND DRUG DELIVERY  
SYSTEMS AGAINST DENGUE

by

JANAE CULMER

B.S., Georgia Southern University, 2020

A Thesis Submitted to the Graduate Faculty of Georgia Southern University in Partial

Fulfillment of the Requirements for the Degree

MASTER OF SCIENCE

© 2022

JANAE CULMER

All Rights Reserved

DEVELOPMENT OF NOVEL PYRIDAZINE DERIVATIVES AND DRUG DELIVERY  
SYSTEMS AGAINST DENGUE

by

JANAE CULMER

Major Professor:  
Committee:

James Carter  
Debanjana Ghosh  
Christine Whitlock

Electronic Version Approved:  
December 2022

## DEDICATION

For my mother, Joycelyn Ann Mackey, for always loving and supporting me

## ACKNOWLEDGEMENTS

The author would like to acknowledge the following for their time and assistance:

Dr. James Carter

My thesis committee, Dr. Debanjana Ghosh and Dr. Christine Whitlock

Dr. Michele McGibony

Dr. Karelle Aiken

Lab Partners: Julissa Rodriguez, Briany Santos, Maxwell Wallace and McKenzie Holmes

## TABLE OF CONTENTS

	PAGE
ACKNOWLEDGMENTS	3
LIST OF TABLES	5
LIST OF FIGURES	6
CHAPTERS	
1. INTRODUCTION	
1.1 THE FIELD OF VIROLOGY	7
1.2 THE OVERVIEW OF FLAVIVIRIDAE	8
1.3 DENGUE AND ZIKA VIRUSES	10
1.4 AEADES MOSQUITO	10
1.5 VIRUS SUPPRESSION METHODS, TREATMENTS AND VACCINES.	11
2. NOVEL PYRIDAZINE DERIVATIVES	
2.1 ANTIVIRAL DRUGS	13
2.2 NOVEL SMALL MOLECULE PYRIDAZINES	13
2.3 PYRIDAZINE DERIVATIVES: PY-LP-3, PY-LP-6, PY-LP-12	15
3. MICELLAR NANOPARTICLES	
3.1 BIODEGRADABLE PH RESPONSIVE COBLOCK POLYMERS	18
3.2 DIBLOCK mPEG-PLA POLYMER	18
3.3 ASSEMBLY AND CHARACTERIZATION OF mPEG-PLA MICELLES	20
4. CELL CULTURE BASED SUPPRESSION	
4.1 VERO CELL LINE	21
4.2 DOSE DEPENDANCE ASSAY	22
4.3 PLAQUE REDUCTION ASSAY	22
5. MATERIALS AND METHODS	
5.1 SYNTHESIS OF NOVEL PYRIDAZINE DERIVATIVES	24
5.2 DOSE DEPENDANCE ASSAY	26
5.3 VIRUS TITRATION USING PLAQUE REDUCTION ASSAY	27
5.4 SYNTHESIS OF DIBLOCK POLYMER, mPEG-PLA	28
5.5 SYNTHESIS OF mPEG-PLA MICELLES	29
6. RESULTS	30
7. DISCUSSION	40
8. CONCLUSION AND FUTURE OUTLOOK	43
9. REFERNCES	44



## LIST OF TABLES

	PAGE
Table 1: Reagents and the amounts utilized to synthesis ionic liquid	24
Table 2: Pyridazine Derivatives along with their chemical names and structures	25
Table 3: Cell type, infection period and incubation time of pyridazine derivatives	28

## LIST OF FIGURES

	PAGE
FIGURE 1: Typical Flavivirus virus diagram	8
FIGURE 2: Life cycle of the Flaviviridae family of viruses	9
FIGURE 3: Map representing the potential range of <i>Flaviviridae</i> mosquitoes in the US	11
FIGURE 4: Structure for pyridazine	14
FIGURE 5: Pyridazine Derivative, PY-LP-3	15
FIGURE 6: Pyridazine Derivative, PY-LP-6	16
FIGURE 7: Pyridazine Derivative, PY-LP-12	16
FIGURE 8: Formation of a biodegradable AB diblock co-polymer	19
FIGURE 9: AB diblock formation via ring-opening polymerization	19
FIGURE 10: AB diblock polymer based, drug-loaded micelles	20
FIGURE 11: Microscopic Image of Vero Cells	21
FIGURE 12: Schematic diagram of a 6-well cell culture	26
FIGURE 13: Schematic diagram of a serial dilution plan for plaque assay	27
FIGURE 14: Schematic representation of 10-fold serial dilution samples dilutions	28
FIGURE 15: Control plate showcasing the effects of no virus/no drug infection	31
FIGURE 16: Plaque Reduction Assay of PY-LP-3	32
FIGURE 17: Plaque Reduction Assay of PY-LP-6	32
FIGURE 18: Plaque Reduction Assay of PY-LP-12	33
FIGURE 19: FT-IR analysis of methoxypolyethylene glycol and D,L-Lactide	34
FIGURE 20: FT-IR analysis of complete diblock polymer, mPEG-PLA	35
FIGURE 21: UV-visual spectroscopy of mPEG-PLA blanks micelles	36
FIGURE 22: Zeta potential of mPEG-PLA micelles	37
FIGURE 23: Average diameter of mPEG-PLA micelles	38
FIGURE 24: Plaque Reduction Assay of mPEG-PLA nanoparticles vs. Zika	39

## CHAPTER 1

### INTRODUCTION

#### 1.1 The Field of Virology

Virology is an extremely broad topic which focuses on subjects such as biology, animal welfare, agriculture and ecology.<sup>1</sup> It is a branch of science that studies viruses and virus-like organisms including their detection, classification, structure, life cycle, isolation, replication, disease-producing properties, cultivation and their use in research and therapies.<sup>1</sup> The main motivation for the study of viruses is due to the myriad number of diseases they cause. Common diseases that viruses are responsible for include: HIV/AIDS, chickenpox, herpes, mumps, measles, shingles, the common cold and flu and Coronavirus disease. It is through virology that scientists can recognize, investigate, and diagnose viral infections along with establishing relationships between the virus, antiviral drugs and the pharmacological responses produced.<sup>1</sup>

Two scientists, Dmitri Ivanovsky and Martinus Beijerinck are credited for their contribution to the discovery of the virus.<sup>2</sup> In 1892, Ivanovsky was investigating a disease in tobacco plants known as the Tobacco Mosaic Disease. It was known by this name due to the transformation of green tobacco leaves to discolored leaves with a mosaic-like pattern.<sup>2</sup> Ivanovsky knew that this incident was caused by a small infectious agent which was not bacteria. Six years later, Beijerinck carried out similar experiments on tobacco plants and named the “small infectious agent”, a virus.

A virus is an infectious microbe that consists of a segment of genetic material surrounded by a bilayer protein coat (Figure 1). Viral genomes are very diverse, as they may contain DNA or RNA, be single or double-stranded, linear, circular, and be various lengths.<sup>3</sup> A virus cannot replicate alone. Instead, it must infect cells and use components of the host cell to make copies of

itself. Most times, a virus kills the host cell in the process, causing damage to the host organism.<sup>3</sup> Viruses have short generation times and relatively high mutation rates.<sup>4</sup> This elevated mutation rate is what allows viruses to rapidly adapt to changes in their host environment. The lack of proofreading skills in the RNA polymerase, which is responsible for copying the virus's genes contributes to this. Viruses can infect all forms of living organisms including animals, plants fungi, bacteria and archaea.

Viruses are categorized at several hierarchical levels of order, family, subfamily, genus, and species based on shared characteristics. There are currently more than 3,600 species, 164 genera, and 71 families comprised of more than 30,000 distinct viral isolates.<sup>3,4</sup> Viruses are divided into families according to their size, shape, chemical makeup, genomic structure, and method of replication.<sup>4</sup>

## 1.2 Overview of *Flaviviridae*

The name *Flaviviridae*, which means "yellow" in Latin, honors the yellow fever virus, which was discovered in Cuba.<sup>5</sup> The members of this virus family, which was composed primarily of

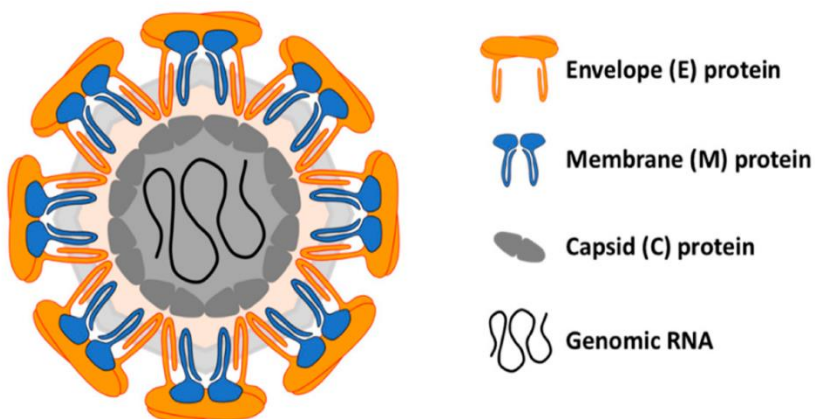


**Figure 1:** Typical Flavivirus virus diagram showing the exterior protein layer encasing the viral RNA<sup>5</sup>

positive-stranded RNA viruses, were grouped into the Flavivirus, Pestivirus, and Hepacivirus superfamilies. *Flaviviridae* are classified according to a small number of fundamental similarities in viral particle properties and replication life cycle. They are

distinguished by a lipid bilayer that encases the nucleocapsid in two or more subunits of the

envelope (E) glycoprotein. The single-stranded RNA genome complex of the nucleocapsid is made up of several basic capsid (C) proteins. (Figure 1).<sup>5</sup>

Receptor-mediated endocytosis is the first step in the general replication of the *Flaviviridae* family of viruses. The virus fuses with the endosomal membrane and releases itself into the cytoplasm. It then breaks apart releasing the viral genome. Viral RNA is translated into a single polypeptide and then replicated. Virus assembly occurs on the surface of the

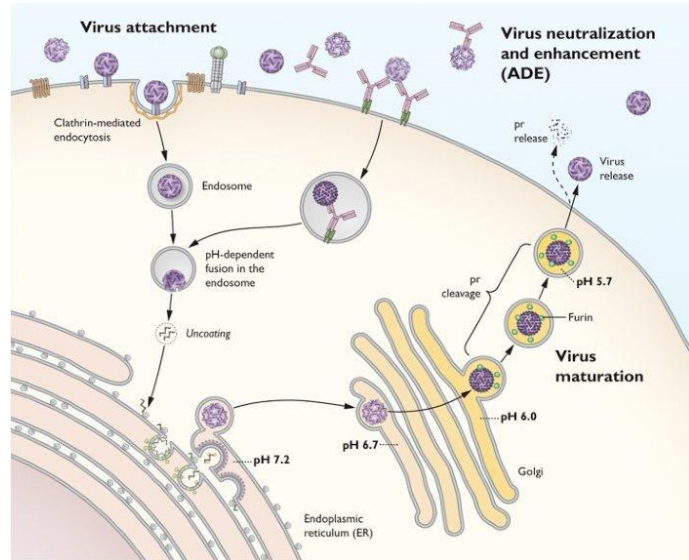


**Figure 2:** Life cycle of the *Flaviviridae* family of viruses<sup>7</sup>

endoplasmic reticulum and newly synthesized RNA buds out. Immature viral particles are then transported through the trans-Golgi network where they mature and convert to their infectious form. Mature viruses will then go on to infect other cells. <sup>6</sup> Figure 2 showcases the replication pathway of *Flaviviridae* viruses.

There are more than 50 species of viruses in the *Flavivirus* genus of the *Flaviviridae* family, the majority of which are arthropod-borne human infections.<sup>1,5</sup> The infectious particles typically have a shape that is nearly spherical and have a diameter of about 50 nm.<sup>5</sup> The family of viruses includes pathogens that cause hepatitis, encephalitis, flaccid paralysis, microcephaly, and vascular leakage. This family of viruses is also responsible for mosquito-transmitted diseases such as Yellow Fever, Dengue Fever, Japanese encephalitis, West Nile viruses, and Zika virus.<sup>7</sup>

### **1.3 Dengue and Zika Viruses**

Dengue and Zika viruses are closely related members of the flavivirus genus and are both transmitted to humans via the bites of infected mosquitoes.<sup>9</sup> These viruses have 40% homology within the envelope protein. Dengue virus infection can be asymptomatic or can cause symptoms such as fever, headache, muscle aches, and rash.<sup>10</sup> Severe symptoms include hemorrhagic fever and internal bleeding.<sup>10</sup> Dengue has become quite prevalent in the United States as the CDC reported dengue as a notifiable condition in 2010. Recent outbreaks of dengue in the United States in Florida, Texas and Hawaii have been noted to be sources of local spreading of this disease marking the fact that this is no longer a travel-associated disease.<sup>11</sup> Outbreaks are often characterized by factors such as weather and lifestyle patterns.

Zika virus causes mostly mild disease with symptoms such as fever, rash, and joint pain that typically resolves within a week.<sup>12</sup> If infected with Zika, severe conditions that can develop include Guillain-Barré syndrome, an autoimmune condition affecting the peripheral nerves, and microcephaly in pregnant women where the virus can lead to brain defects in the developing fetus including microcephaly.<sup>13</sup> With a vast portion of the population at risk and symptoms that can seamlessly go unnoticed, the need for targeted therapies is quite clear.

### **1.4 *Aedes* Mosquitoes**

*Aedes albopictus* and *Aedes aegypti* are two mosquito species that frequently serve as the primary vectors for *Flaviviridae* viral illnesses such as Dengue and Zika. These vectors live in tropical, subtropical, and temperate climates.<sup>8</sup> It is only the female mosquito that is responsible for biting therefore they are also responsible for the transmittance of the virus to the host. The *Aedes albopictus* mosquito blood feed on both animals and humans which drops the likelihood of spreading viruses transmittable to humans. The *Aedes aegypti* prefer to feed on human blood,

making them more likely to spread diseases like dengue, West Nile, and Zika that are transmitted by people. The Zika virus is not currently being transmitted locally in the United States. The last instances of regional mosquito-borne Zika transmission in the continental United States were in Florida and Texas in 2016–17, according to the Centers for Disease Control and Prevention. Local dengue epidemics have most recently been reported in Hawaii (2015), Florida (2013, 2020), and Texas in the United States (2013). The majority of outbreaks in the United States have been localized to modestly sized locations.<sup>8</sup> Figure 3 shows the CDC’s best estimate of the potential range of *Aedes aegypti* and *Aedes albopictus* in the contiguous United States.

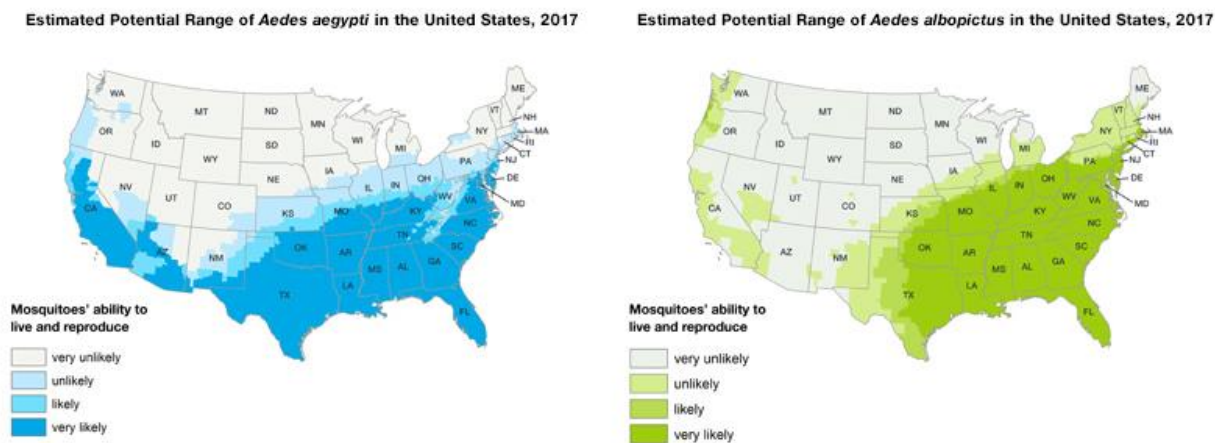


**Figure 3:** Map representing the potential range of *Aedes aegypti* and *Aedes albopictus* in the US<sup>9</sup>

### 1.5 Virus Suppression Methods, Treatments and Vaccines

Vaccines are considered the most effective method for the prevention of virus infection. The process of creating vaccines and antiviral medications may be considered challenging due to the fast capability of a virus to evolve and frequent resistant mutations. Zika currently lacks an approved vaccine whereas Dengue has one known vaccine, Dengvaxia. To formulate this vaccine, the precursor membrane and envelope found in the yellow fever virus were swapped out

for dengue counterparts.<sup>14</sup> The four dengue strains are not all protected by this vaccine. Dengvaxia showcases 34.7% efficiency against DENV2. This strand produces the most serious infection compared to the other strands. Use of this vaccine is only approved for individuals between the ages of 9 to 16 that have had a history of the dengue infection.<sup>13</sup> This leaves others out of this age category at greater risk for fighting off infections of Dengue. Furthermore, given that one research resulted in the deaths of 10 infants, vaccine developers have expressed worries about the efficacy and safety of the vaccine.<sup>15</sup> Following the establishment of virus immunization programs, escape mutants could possibly appear.

Dengue and Zika viruses can simultaneously replicate in the same mosquito populations. The cocirculation of these viruses produces a phenomenon that leads to simultaneous infections of individuals and cross-immunoreactivity of related antibodies.<sup>16,17</sup> The infectivity of one virus enhances the subsequent infection of the other virus which raises awareness for the necessity of vaccines and antiviral medications. The above-mentioned advantages and disadvantages show how urgently small molecule inhibitors and medication delivery systems against viruses need to be developed. As a result, the research that is being presented here is intended to meet these needs.



## CHAPTER 2

### NOVEL PYRIDAZINE DERIVATIVES

#### 2.1 Antiviral Drugs

Antivirals are drugs that help the body fight against dangerous viruses. Antiviral drugs protect organisms from viral infections and the spread of those diseases by taking preventive measures.<sup>18</sup> Its functionality is entirely dependent on the elements of the medicine from which it is made and the virus that it is intended to combat. Antivirals primarily work in three different ways: 1) Disabling receptors prevents the virus from attaching to and infecting healthy living cells. 2) Boosting the immune system enables the organism to fend off viral activity. 3) Reducing the amount of active virus in the organism.<sup>18</sup>

Important variables affecting the frequency and/or severity of viral infections include population density, immunological health, infection vectors and virulence, nutritional condition, cleanliness, genetic vulnerability, and medical management of cases.<sup>19</sup> Thus, the frequency of virus infections, their clinical significance, and the requirement for antiviral medications vary from location to location and from time to time. The availability, safety, cost, and efficacy of alternative approaches, such as the control of infection-carrying vectors, viral vaccine vaccination, or therapy with already-approved antiviral medications, should be considered when developing new antiviral medications.<sup>20</sup> Pyridazine derivative compounds have been shown to showcase antiviral properties.

#### 2.2 Novel Small Molecule Pyridazines

Pyridazines and their derivatives have recently attracted a lot of interest due to the discovery of compounds with potential medical applications.<sup>21</sup> Pyridazines are heteroaromatic, six-membered chemical compounds having a wide range of biological and pharmacological

activity. They play a key structural role in many physiologically active molecules. The pyridazine ring system is a 1, 2- diazine or o- diaza benzene.<sup>21</sup> The diazo group provides significant use as precursors for reactive intermediates.<sup>21</sup>

Due to its imine functional groups, it is an odorless liquid at ambient temperature with a comparatively high boiling point of 208 °C and low melting point of -8 °C. The pyridazine molecule is a pyridine-like heteroaromatic substance.<sup>21</sup> Pyridazine's fundamental aromatic ring structure consists of two nearby nitrogen atoms (Figure 4).

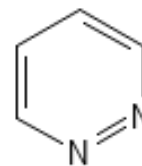


**Figure 4:** Structure for pyridazine

This compound's nitrogen atoms provide special chemistry; they can interact with suitable substrates that have acidic functional groups to produce supramolecular complexes. Additionally, pyridazines have high-efficiency turnover numbers and are efficient water oxidation catalysts.<sup>21,22</sup> Although pyridazines are not used in everyday life, they are primarily used in research and industry as a component of many complex chemical compounds. In addition, pyridazines are helpful intermediates in physical organic chemistry for the synthesis of numerous other heterocycles.<sup>23</sup>

Pyridazines have been found to have a wide range of biological effects, including those that are antibacterial, antibiotic, anti-depressant, anti-diabetic, anti-hypertensive, analgesic, anti-tumor, antiviral, anti-inflammatory, anti-viral, anti-cancer, anti-aggregative, and anti-epileptic. These substances are also used to induce drowsiness, hypnosis, anesthesia, sleep, and muscular relaxation in order to treat sleep problems like insomnia.<sup>24</sup>

Pyridazines are widely used in medication development and interfere with a variety of enzyme regulatory pathways. Due to their structure, stability, and reactivity as well as their

propensity to produce stable compounds with beneficial biological properties, some recently synthesized pyridazine derivatives have found interest in a variety of scientific domains. According to recent studies, dry eye problems, prostate cancer, and dermatosis can all be treated with pyridazine derivatives.<sup>24</sup> Additionally, pyridazines have the ability to conduct electricity. These substances have qualities including low density, good resistance at room temperature, and the ability to be stretched to create thin films. These conductive polymers can also be incorporated into nanoparticles.<sup>25</sup>

### 2.3 Pyridazine Derivatives: PY-LP-3, PY-LP-6 and PY-LP-12

Three (3) novel small molecule microwave-assisted pyridazine derivatives were synthesized from the lab of Dr. Shainaz Landge. The derivatives have similar structures and differ in the phenyl substituent. These positionings give us useful information on the binding position while allowing us to experiment with the system's electronics. It will also direct us as to which group should be given preference for electronic donations and withdrawals in order for the system to function. The pyridazine derivatives are shown and described below:

Derivative PY-LP-3 has a chemical name of 3-(5,6-diphenylpyridazin-3-yl) with a chemical formula of  $C_{22}H_{17}N_3$  and a molecular weight of 323.40 g/mol. The functional group belonging to this derivative is the amino group,  $-NH_2$ , which is meta-positioned on a benzene ring (Figure 5). Consisting of a phenyl group attached to an amino group, aniline is formed. By itself it is the simplest aromatic amine. When stable, aniline is mainly used for the preparation of analgesics,

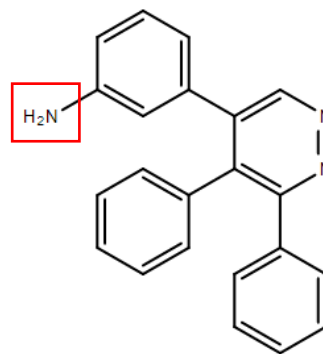


**Figure 5:** Structure of Pyridazine Derivative, PY-LP-3 with emphasis placed on the meta-positioned amino functional group

antipyretics, antiallergics, and vitamins.<sup>26</sup> Examples of known drugs that contain aminobenzene are sulfamethizole which is an antibiotic used to treat a wide variety of susceptible bacterial infections, sulfadoxine which is a long-acting sulfonamide used for the treatment or prevention of malaria and bicalutamide which is used as a receptor inhibitor to treat Stage D2 metastatic carcinoma of the prostate.<sup>27</sup>

PY-LP-6 has a chemical name of 5-(4-chlorophenyl)-3,4-diphenylpyridazine with a chemical formula of  $C_{22}H_{15}ClN_2$  and a molecular weight of 342.83 g/mol. The functional group belonging to this derivative is the chloro group, -Cl,

which is para-positioned on a benzene ring. The reactivity of chlorobenzene is low when compared to other para directors attached to benzene rings. This is due to the high

electronegativity of the chlorine atom. It is electron

withdrawing so reduces the electron density of the ring. In the

pharmaceutical industry, chlorobenzene is used in the

synthesis of vitamin B6 and in the synthesis of drugs for epilepsy, thyroid and liver cancer.<sup>28</sup>

Derivative PY-LP-12 has a chemical name of 6-(4-methoxyphenyl)-3,4-

diphenylpyridazine with a chemical formula of  $C_{23}H_{18}N_2O$  and a molecular weight of 338.41 g/mol. The functional group

belonging to this derivative is the methoxy group, -OCH<sub>3</sub>, which

is para-positioned on a benzene ring. Methoxy is also considered

an electron withdrawing group due to the electronegativity of

oxygen. The functional group itself is included in many

helpful drugs. These include: methoxyflurane which is used to

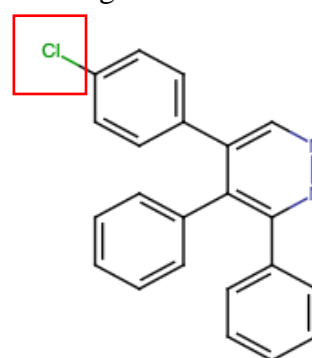


**Figure 6:** Structure of Pyridazine Derivative, PY-LP-6 with emphasis placed on the para-positioned chloro functional group

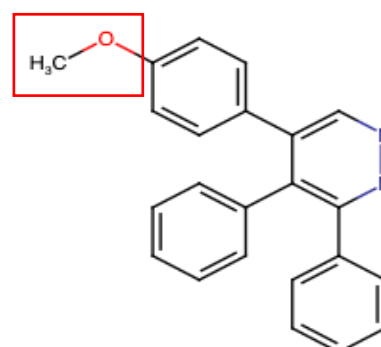


**Figure 7:** Structure of Pyridazine Derivative, PY-LP-12 with emphasis placed on the para-positioned methoxy functional group

ease pain and methoxy polyethylene glycol-epoetin which is an injection used to treat anemia and chronic kidney failure.<sup>29</sup>

All the pyridazine derivatives underwent initial cell culture-based suppression assays, dose dependent assays and viral titration via plaque assay. Those showcasing viral suppression will then be drug loaded into mPEG-PLA nanoparticles. Due to a production shortage of these derivatives, drug-loading was not executed. Upon gaining further supply of these derivatives, drug-loading is in future perspective.

## CHAPTER 3

### MICELLAR NANOPARTICLES

#### **3.1 Biodegradable pH Responsive Coblock Polymers**

Due to their numerous uses, biodegradable polymers have recently attracted attention for usage in biological applications. Biocompatible polymers may now be assembled into functional nano-sized units thanks to special characteristics, expanding their therapeutic applications. These biodegradable polymers are advantageous for biomedical applications because they are quickly broken down, absorbed, or removed in a human body after serving their purpose.<sup>30</sup>

Drug formulation uses biodegradable co-block polymers in a variety of ways. Biocompatible monomers that are deliberately chosen for beneficial qualities, such as medication solubility and dissociation, are combined by scientists. Since amphiphilic block copolymers have been recognized to self-assemble to create polymeric micelles under particular concentrations, they combine into copolymers and enable researchers to investigate their biological applications, including drug delivery systems. In relation to my research, proposed micellar nanoparticles and related antivirals will help in identifying pH-microenvironments within infected cells that can aid in drug delivery leading to a novel method for the suppression of viruses.

#### **3.2 Diblock mPEG-PLA Polymer**

A and B are the two types of monomers that make up a diblock copolymer, a polymer. When two monomer chains are grafted together to make a single copolymer chain, the monomers are ordered so that each monomer has its own chain.<sup>31</sup> Methoxypolyethylene glycol (mPEG) and polylactide are the two segments that are connected to produce the single diblock strand that gives the polymer chain, mPEG-PLA, its name. Polymer segment patterns are

frequently shortened to alphabetic patterns that give each individual monomer unit a letter. The designated letters for the mPEG-PLA polymer would be "AB" (Figure 8). The "A" units in this case relate to the mPEG that caps the polylactide "B" unit. The A monomer coupled to the B monomer forms the diblock, mPEG-PLA.

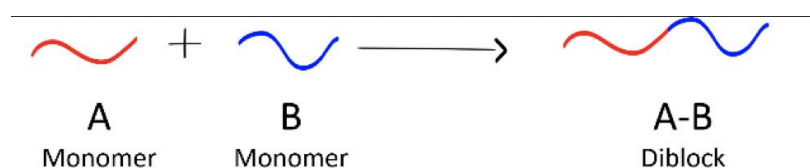


**Figure 8:** Schematic illustration depicting the formation of a biodegradable AB diblock co-polymer



**Figure 9:** AB diblock formation via ring-opening polymerization of D,L-lactide and methoxypolyethylene glycol<sup>32</sup>

By employing mPEG as an initiator and stannous octoate [Sn(Oct)<sub>2</sub>] as a catalyst, ring-opening polymerization of D,L-lactide results in the polymerization of the AB diblock (Figure 9). Methoxypolyethylene glycol and polylactide are two specific polymers that are utilized in numerous medicines and are listed in the FDA's criteria for commercially available inactive components.<sup>32</sup> The created diblock, mPEG-PLA, has a special ability to undergo thermally induced self-assembly without the need of harsh solvents. The solvent can stay biocompatible and pH-specific by carefully lining up under unique heating conditions, allowing the polymer to target the acid-catalyzed fusion of the virus and endosome where viral RNA is released and started for replication in the endoplasmic reticulum. The AB diblock polymer is attractive as a

potential medication delivery method because of its beneficial biodegradable and nontoxic qualities.<sup>33</sup>

### 3.3 Assembly and Characterization of mPEG-PLA Micelles

Amphiphilic characteristics are present in mPEG-PLA copolymer as it contains both hydrophobic and hydrophilic regions. When micelles form in a solution, the hydrophilic mPEG chain segment forms the outer micelles, and the hydrophobic PLA chain segment forms the inner micelles.<sup>34</sup> Due to self-assembly into polymeric micelles in an aqueous solution, this property of copolymer materials can be utilized to boost the solubility of some insoluble pharmaceuticals.<sup>34, 35</sup> Thermally induced self-assembly forms spherical shells that can be used as carriers when the polymer is exposed to a sudden change in temperature (Figure 10). In a biologically friendly solvent, such as ultra-pure water, these micelles can be formed.

Prepared mPEG-PLA nanoparticles should be spherical in shape with a size less than 100 nm.<sup>36</sup> Surface charge and surface chemistry and size distribution are all investigated by dynamic light scattering and Zeta-potential analyzer.

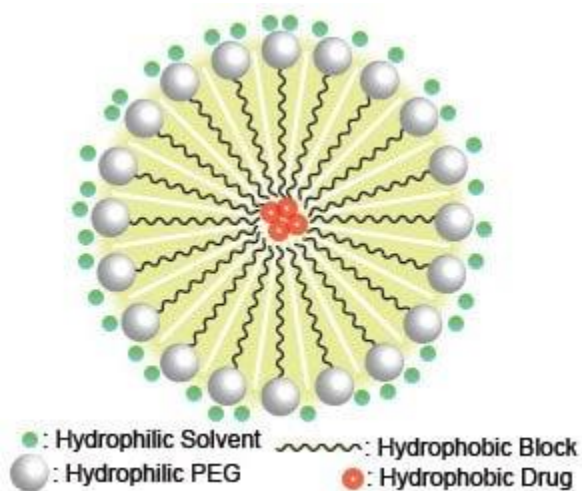


**Figure 10:** AB diblock polymer based, drug-loaded micelles<sup>36</sup>



## CHAPTER 4

## CELL CULTURE BASED SUPPRESSION

**4.1 Vero Cell Line**

Derived from the kidney of an African green monkey (*Cercopithecus aethiops*) in the 1960s, Vero cells are among the most widely used mammalian cell lines in science, particularly in virology experiments.<sup>37</sup> They are anchorage-dependent cells as they are unable to divide or survive without being affixed to a surface. Lacking the ability to make interferon alpha or beta due to a loss in type I interferon genes, they have increased susceptibility to viral infection. Numerous viruses, including the simian polyoma virus SV-40, measles, rubella, arboviruses, adenoviruses, influenza virus, and Ebola hemorrhagic fever virus have been studied using Vero cells.<sup>38</sup>

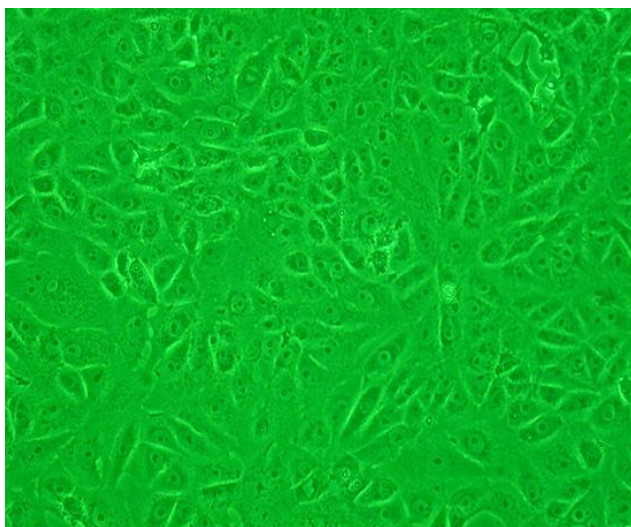


**Figure 11:** Microscopic Image of Vero Cells under Green Light at 100-fold magnification<sup>38</sup>

Vero cells have the following advantages. Firstly, the cell bank is easy to establish and preserve, at the same time it can be continuously passaged with a fast growth rate. Secondly, Vero cells have stable genetic traits and a low probability of malignancy. Thirdly, Vero cells are sensitive to a variety of viruses and have high virus titers.<sup>39</sup> Finally, Vero cells could exceedingly be resistant to various cultural conditions, and the requirements are not high that it can grow well on the surface of the microcarrier, which proves that Vero cells have significant value in the development of a series of viral vaccines.<sup>39</sup>

## 4.2 Dose Dependence Assay

Dose-response assays are a popular and often used technique that evaluates the toxicity of prospective drug targets on cell test populations.<sup>40</sup> These tests often entail applying successive dilutions of the test substances such as drug to cell samples in order to assess the level of cell activity over a wide range of doses.

An effective dose is predicated on the ideas of IC<sub>50</sub> and EC<sub>50</sub>. The pharmacological concentration at which half-maximal reaction occurs is known as the EC<sub>50</sub>. The inhibitory concentration (IC<sub>50</sub>) is the level at which the response (or binding) is reduced by 50%. The most generally used and useful indicator of a drug's effectiveness is its half-maximal inhibitory concentration (IC<sub>50</sub>). It provides a gauge of the potency of an drug in pharmacological research by indicating the amount of drug required to block a biological process by 50%. As a toxicity gauge, EC<sub>50</sub> is used.<sup>41</sup> Calculations of IC<sub>50</sub> and EC<sub>50</sub> are possible after quantitation by plaque reduction assay.

## 4.3 Plaque Reduction Assay

A trusted technique for determining viral concentration in relation to infectious dose is the plaque assay. To perform the assay, a monolayer of virus-infected cells must be counted to determine how many plaque forming units (pfu) were generated. Crystal violet staining of the preserved cell monolayer allows for the visualization of plaques.<sup>42</sup>

Cultured cells that can be infected by the target virus are needed for plaque assays. After being seeded onto a surface that will allow them to adhere and develop, the cells are permitted to form a confluent monolayer. The next step involves diluting a viral sample numerous times before adding it to a 24-well plate containing cells. Infected cells that are killed by the virus

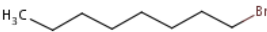
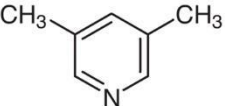
separate and break the monolayer through lysis or other processes. On the growing surface, these areas—which are now empty of cells—appear as round spots and are referred to as plaques.

## CHAPTER 5

## MATERIAL AND METHODS

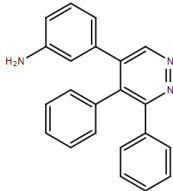
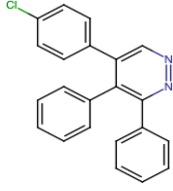
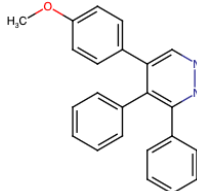
## 5.1 Synthesis of Novel Pyridazine Derivatives

A total of three (3) organic compounds were previously synthesized for the purpose of this research project via collaboration with Dr. Shainaz Landge. The microwave assisted synthesis of these derivatives first began with the synthesis of ionic liquid, 1-n-octyl-3,5-dimethylpyridinium bromide. Its preparation consisted of two reagents, n-octyl bromide and 3,5-lutidine (Table 2). Once mixed, continuous stirring took place for a total of twenty (20) hours in a dark environment until a yellow liquid has been formed. Vacuum filtration was also carried out and the ionic liquid was stored in a desiccator until use.

CHEMICAL	MOLECULAR WEIGHT (g)	MOLARITY	MASS (g)	VOLUME (mL)	DENSITY (g/L)	EQUIVALENCE
 n-octyl bromide	107.15	0.1	10.715	11.41	0.939	1
 3,5-lutidine	193.128	0.1	19.312 8	17.34	1.114	1

**Table 1:** Reagents and the amounts utilized to synthesis 1-n-octyl-3,5-dimethylpyridinium, ionic liquid

In order to synthesize each of the pyridazine derivatives (Table 3), five reagents were used in various quantities each unique to each derivative. These reagents consisted of benzil, acetophenone (methyl, amino, chloro, or fluoro), hydrazine hydrate, 4-tetra-butyl ammonium, prepared ionic liquid and ethanol to dissolve solids. Once combined, the mixture was stirred overnight in a round bottom flask completely covered with foil to prevent light from interfering with the reaction. After stirring, cold DI water was added to precipitate the reaction. Characterization via Nuclear Magnetic Resonance (NMR) was completed to confirm that the compounds had cyclized. Once cyclized, purification was done through column chromatography techniques. As previously stated, synthesis of novel pyridazines derivatives were prepared via a collaborator therefore, this research does not give details regarding its characterization and optimization.

	Chemical Name	Structure
PY-LP-3	3-(5,6-diphenylpyridazin-3-yl)aniline	
PY-LP-6	5-(4-chlorophenyl)-3,4-diphenylpyridazine	
PY-LP-12	6-(4-methoxyphenyl)-3,4-diphenylpyridazine	

**Table 2:** Pyridazine Derivatives along with their chemical names and structures

## 5.2 Dose Dependence Assay

Pyridazine derivatives products PY-LP-3, PY-LP-6 and PY-LP-12 were used for analysis of cell culture-based suppression. 0.11g -0.12g of each drug was dissolved in dimethylsulfoxide (DMSO) and then transferred to a 50 mL conical flask. Dulbecco's Modified Eagle Medium (DMEM) containing 10% Fetal Bovine Serum (FBS) was also added to the 50 mL mark. The

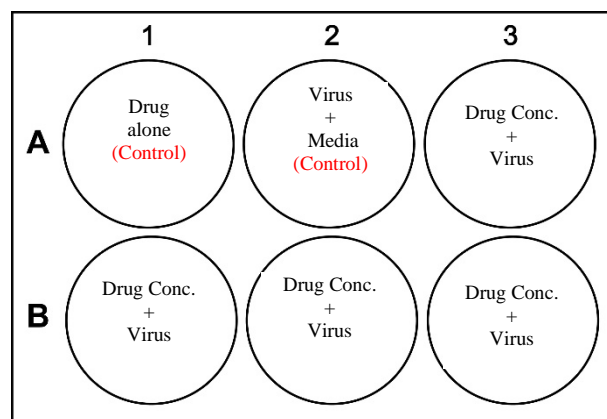


**Figure 12:** Schematic diagram of a 6-well cell culture plate that showcases placement of control sample and samples containing various concentrations of drug.

working concentration of PY-LP-3, LY-LP-6 and PY-LP-12 were calculated to be, respectfully: 33.3 mg/mL, 27.6 mg/mL and 27.5 mg/mL. In 6 well plates, Vero cells were plated and left to incubate for a total of 24 hours to allow for cell bonding to well surface.

Following this incubation period, a dose-dependent assay was performed. Using a 2 mL aspirating pipette, media was aspirated

from the wells. The cells were then washed twice with 0.5 mL of Phosphate Buffered Saline (PBS) with aspiration between washes. The cells were then overlaid with 0.5 mL DMEM containing 2% FBS, which possessed 50  $\mu$ L of Zika virus. Zika virus was used in the testing of potential suppression by the pyridazine derivatives due to initial issues growing dengue virus stocks. We suspect this is due to suspect samples that were obtained from the American Type Culture Collection (ATCC), a global biological resource center that collects, stores and distributes microorganisms, cell lines and other research material. The appropriate amount of drug and virus were added into the wells except for the negative control and drug only wells (Figure 13). The 6 well plates were placed in 37 degrees Celsius, 5% CO<sub>2</sub> incubator for 1 hour

whilst being rocked/tilted every 15 minutes. After the hour, media was aspirated from the wells and the respective contents were added back into each well excluding the addition of virus. The cell plate was then incubated for two days. After the incubation period, the cell culture fluids were collected and stored at -80 degrees Celsius for future analysis by plaque assay. This same procedure was also utilized for the addition of nanoparticles/micelles against virus.

### 5.3 Virus Titration Using Plaque Reduction Assay

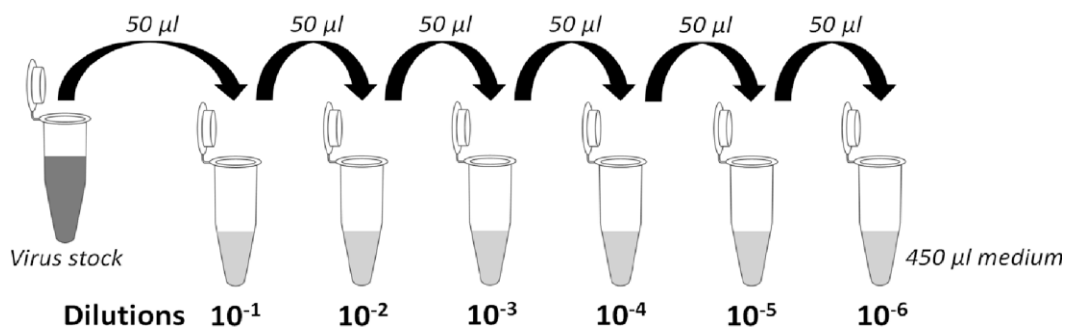


**Figure 13:** Schematic diagram of a serial dilution plan for plaque assay

First, virus titration consisted of setting up serial dilutions from the cell culture fluid stocks that were previously collected and stored from the dose-dependent assay. Ten fold serial dilutions was the method used to make these dilutions, with each microtube containing 450 µl of DMEM (Figure 14). Using a pipette, 50 µl of virus sample from the stock was placed in the first microtube, labeled 10<sup>-1</sup> and vortexed for ~3 seconds. From the microtube labeled 10<sup>-1</sup>, 50 µl of that sample was transferred into the second microtube, labeled 10<sup>-2</sup> and vortexed. This process was then repeated for the remaining dilutions, 10<sup>-3</sup> to 10<sup>-6</sup> as seen in **Figure 15**. To avoid cross contamination, pipette tips were changed between dilutions. The day prior to the assay, Vero cells were plated in a 24-well plate to prepare for the addition of the samples containing the serial dilutions. Each column of the plate was aspirated of its media and the samples from the

microtube were gently added in each respectively well. The cells were then incubated at 37°C for 5 days.

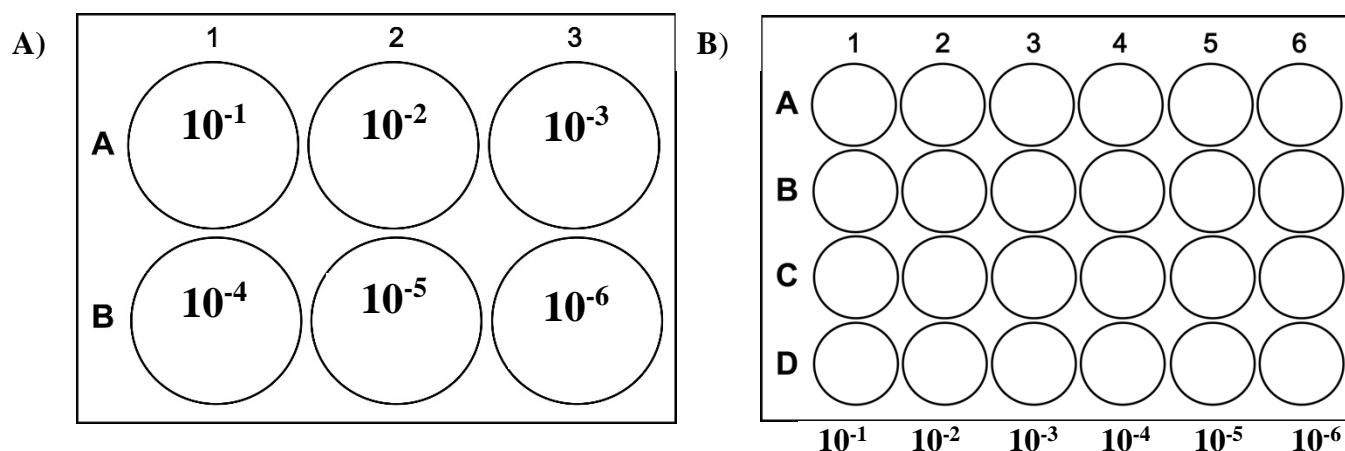


**Figure 14:** Schematic representation of 10-fold serial dilution samples dilutions from respective wells of 6-well plates (Panel A) into 24 well plates (Panel B)

After the 5 day incubation period, the wells were aspirated and 0.05% crystal violet in 10% formalin was added fix and stain cells. The plate was then incubated for 30 minutes at room temperature and crystal violet staining solution was removed via aspiration. The cells were then washed 1 to 2 times with tap water to aid in the visualization and quantitation of plaques which indicate viral infection.

#### 5.4 Synthesis of diblock polymer, mPEG-PLA

The synthesis of mPEG-PLA diblock polymer occurs through ring-opening polymerization of D,L-lactide which uses mPEG as an initiator and stannous octate as a catalyst. Under a protective nitrogen atmosphere, 2 grams of mPEG, 1 gram of D, L-lactide and 100  $\mu$ L of stannous octate were mixed at 140 °C for 4 hours. Once refluxed, the product was purified by dissolution in dichloromethane, precipitated in diethyl ether and then dried overnight. The final product was then lyophilized (LABCONCO FreeZone 4.5 Plus) and then stored at -20°C until



characterization on Fourier-transform infrared spectroscopy (Thermo Scientific Nicolet iS10) or until further use.

### **5.5 Synthesis of mPEG-PLA Micelles**

To synthesize blank micelles of mPEG-PLA, its previous lyophilized product was dissolved in ultrapure DI water (18.2 MW cm at 25°C) at a ratio of 20 mg of polymer in 1 mL of water and placed in a water bath (Thermo Scientific Precision CIR 19) at 37°C for 4 hours. Once thermal induced self-assembly of the micelles is complete, the solution is filtered through a 0.2 µm syringe filter (Corning sterile syringe filter). The filtrate containing blank micelles is then characterized using UV-Visual spectroscopy (Shimadzu UV-2600 UV-VIS Spectrophotometer) and dynamic light scattering (Malvern Nano series NANO-ZS ZetaSizer) to ensure that the micelles were fully formed.

## CHAPTER 6

## RESULTS

**6.1 Cell Culture Based Suppression of PY-LP-3, PY-LP-6 and PY-LP-12**

All three of the named pyridazine derivatives underwent cell culture suppression assays. Representative results were derived from viral titration via plaque assay. Plaque assays' ability to accurately measure viral titers depends on a number of variables, including the selection of the correct host cells, media and growth conditions for cellular and viral viability and a precise estimation of the viral incubation period to allow enough time for distinct and countable plaque formation.<sup>43</sup> **Table 4** provides information on the host cells, duration of the infection period with Zika virus and the incubation time allowed for plaque formation.

	PY-LP-3	PY-LP-6	PY-LP-12
Cell Type	Vero	Vero	Vero
Infection period	1hr	1hr	1hr
Incubation Time	3-5 days	5 days	5 days

**Table 3:** Cell type, infection period and incubation time of PY-LP-3, PY-LP-6 and PY-LP-12

After the initial infection and application of an immobilizing overlay which is carboxymethyl cellulose (CMC), individual plaques will start to develop as viral infection and replication are constrained to the surrounding monolayer. CMC allows plaques to form because it greatly decreases viral spread. After incubation, cells are stained to enhance the contrast between plaques and the uninfected monolayer. Plaques are then enumerated and used to

calculate the titer of infectious virus in the specimen. When enumerated, plaques were distinct and countable to the naked eye.

The following formula is used to determine virus titer:

$$\text{Number of plaques} \times (D \times V) = \text{pfu/mL}$$

D = dilution factor

V = Volume of diluted virus/well

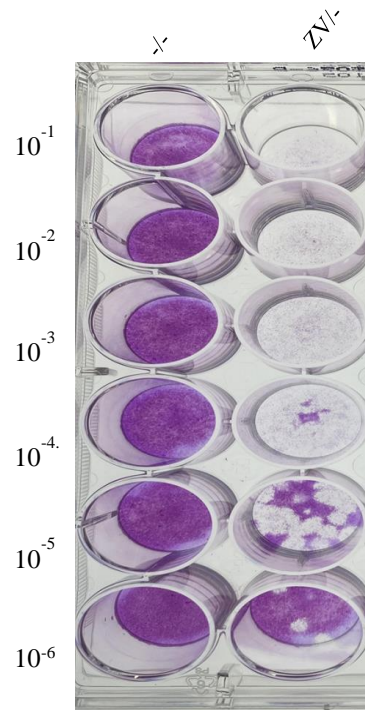


**Figure 15:** Control plate showcasing the effects of no virus/no drug infection and virus/no drug infection

ZV/20    ZV/15    ZV/10    ZV/5

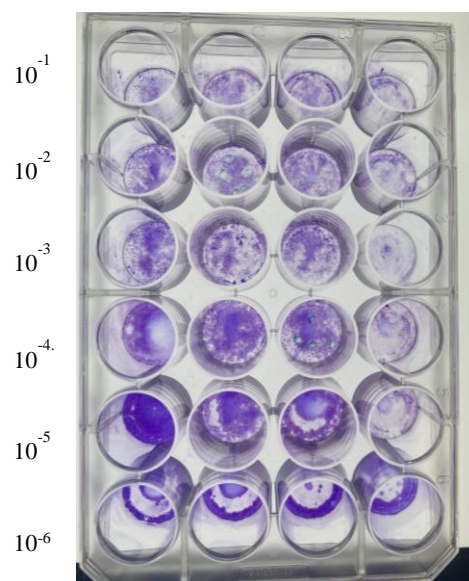


**Figure 16:** Vero cells were plated at  $0.24 \times 10^6$  cells and infected with Zika virus using 10-fold serial dilutions against pyridazine derivative, PY-LP-3. (MOI = 1.0). Plaques were counted and titered.

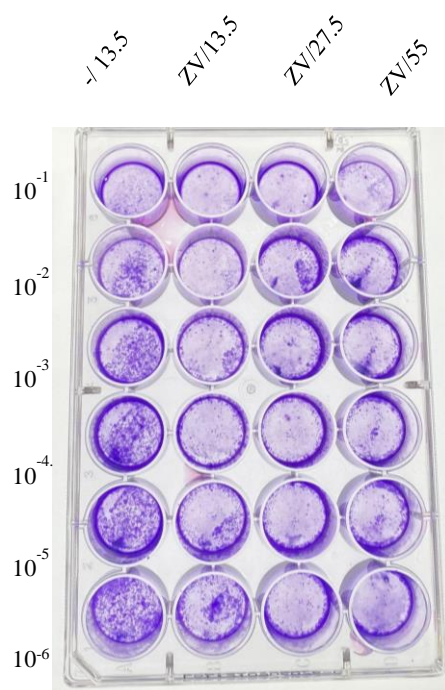


**Figure 17:** Vero cells were plated at  $0.24 \times 10^6$  cells and infected with Zika virus using 10-fold serial dilutions against pyridazine derivative, PY-LP-6. (MOI = 1.0). Plaques were unable to counted and tittered for due to large amount of cell death.

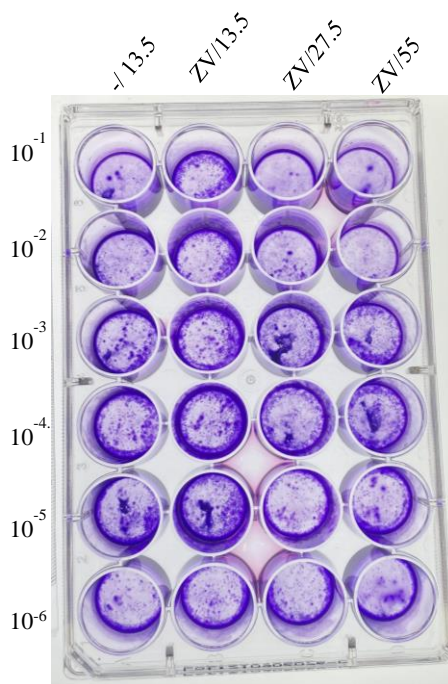


**Figure 18:** Vero cells were plated at  $0.24 \times 10^6$  cells and infected with Zika virus using 10-fold serial dilutions against pyridazine derivative, PY-LP-12. (MOI = 1.0). Plaques were unable to counted and tittered for due to large amount of cell death.

## 6.2 Characterization of diblock polymer, mPEG-PLA

Fourier-transform infrared spectroscopy, or FTIR, was carried out on the AB diblock to confirm proper diblock production (Figure 20). The two segments were verified by comparing the FTIR peaks to values from the literature. The peak found around  $2900 \text{ cm}^{-1}$  is due to CH stretching seen in the mPEG segments. The peak around  $1750 \text{ cm}^{-1}$  in the diblock polymer reveals the existence of the esters in the PLA segment. Peaks at  $1000 \text{ cm}^{-1}$  in the fingerprint area contributes to ether stretching. (Figure 19)

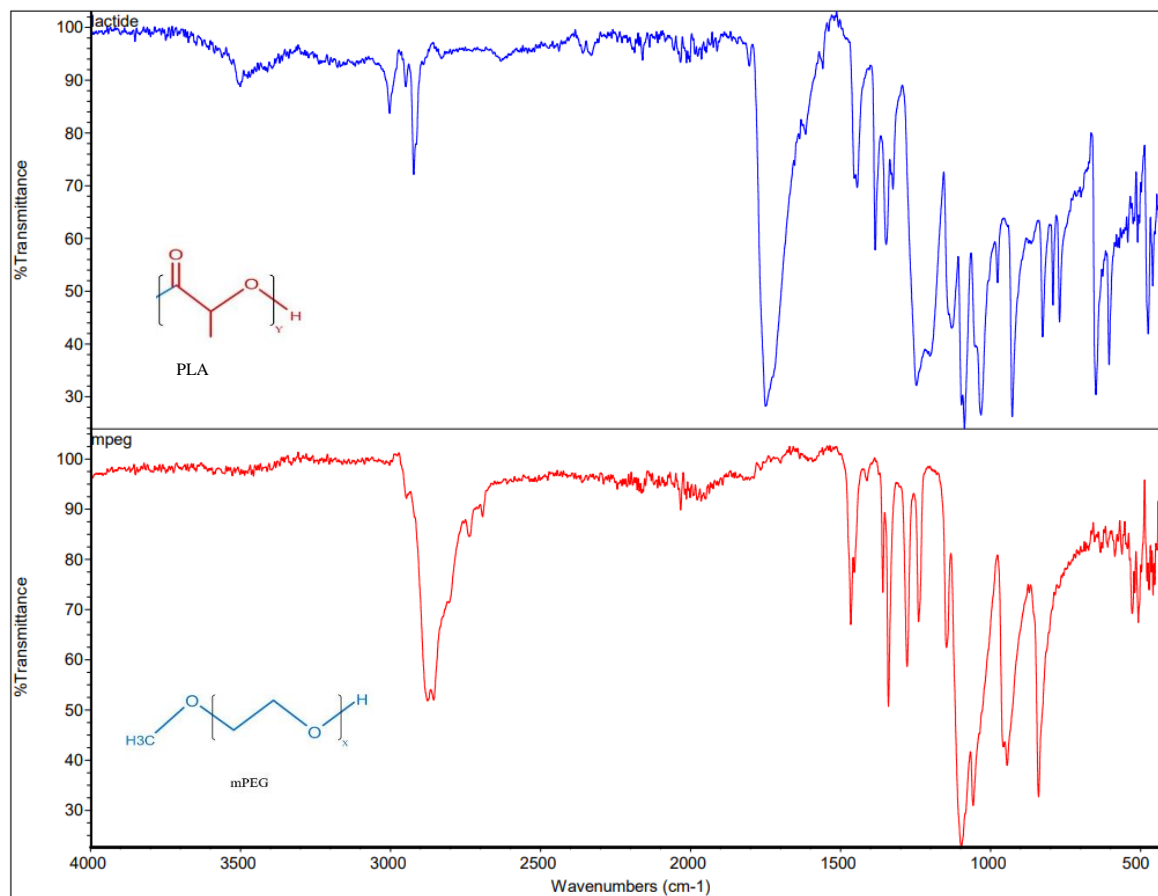


**Figure 19:** FT-IR analysis of methoxypolyethylene glycol (mPEG) and D,L-Lactide (PLA)

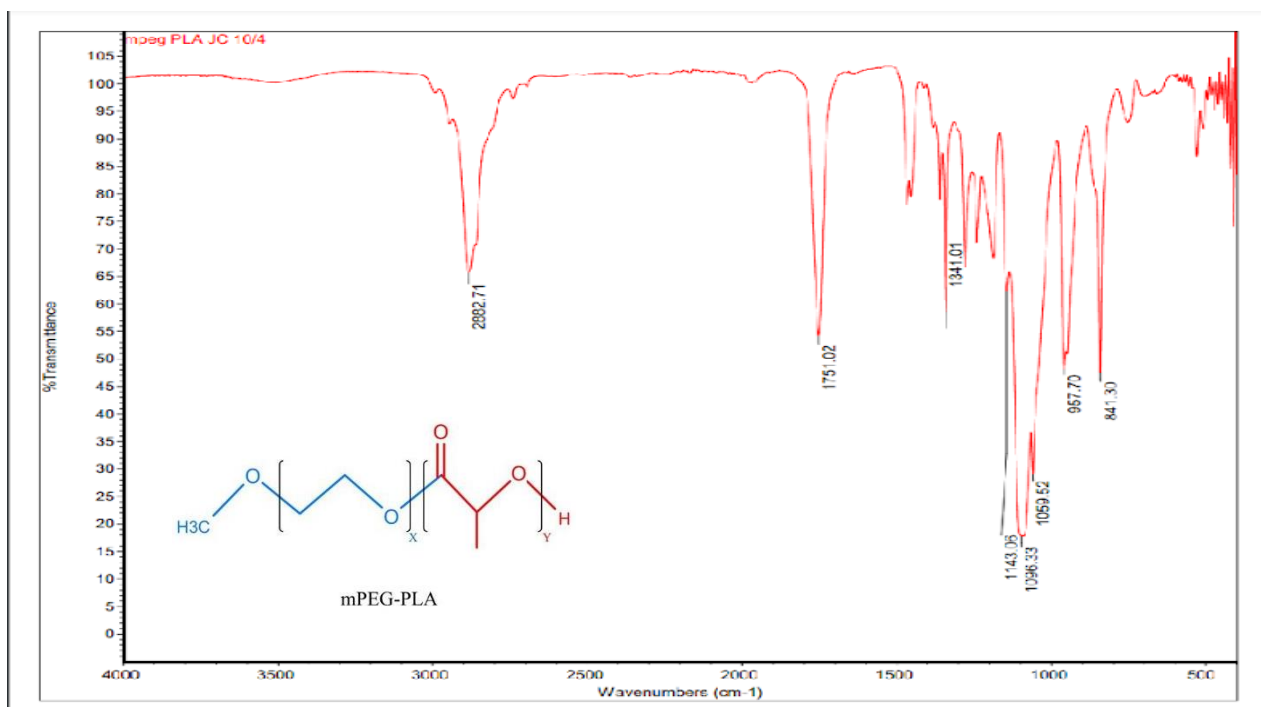


**Figure 20:** FT-IR analysis of complete diblock polymer, mPEG-PLA.

### 6.3 Characterization of diblock polymer, mPEG-PLA micelles

Due to a shortage of supply of pyridazine derivatives PY-LP-3, PY-LP-6 and PY-LP-12, mPEG-PLA micelles were unable to be drug loaded. Therefore, after being thermally induced for self-assembly and filtered, polymer based micelles without any drugs loaded into them, also known as blanks were characterized via UV-visual spectroscopy and to ensure micelle formation. Figure 19 shows the spectra of mPEG-PLA blanks where there is a distinct peak occurring around 310 nm.

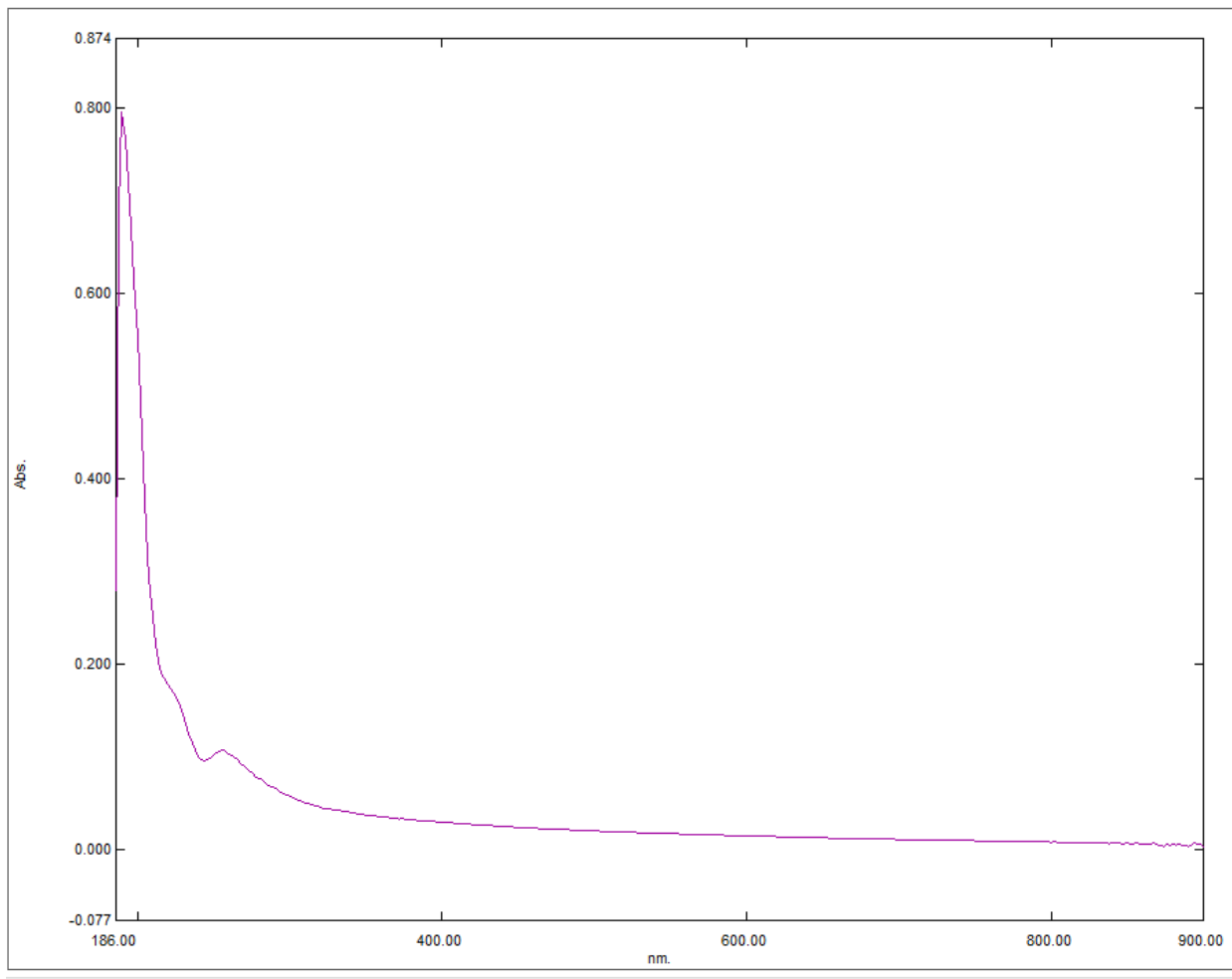


**Figure 21:** UV-visual spectroscopy of mPEG-PLA blank micelles suspended in ultra-pure DI water

As an initial assessment of co-polymer assembly into biodegradable micellar nanoparticles, additional characterization of the blank micelles was carried out. Micelle surface charge was determined using the zeta potential method, and the average diameter of each micelle particle in suspension was determined using dynamic light scattering. These measurements were used to predict strong repulsive or attractive forces that might arise when the micelles are tested *in vitro*. The zeta potential of micelles is -1.44 mV (Figure 20) while the average diameter of the micelles is 78.96 nm (Figure 21).



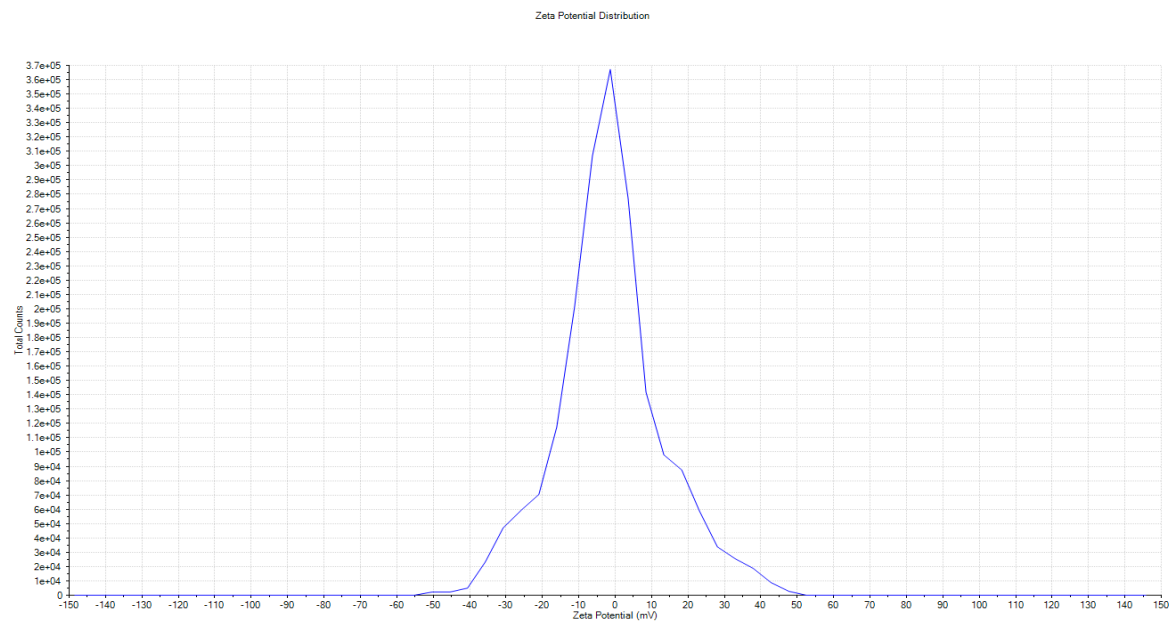


**Figure 22:** Zeta potential of mPEG-PLA micelles suspended in ultra-pure DI water.

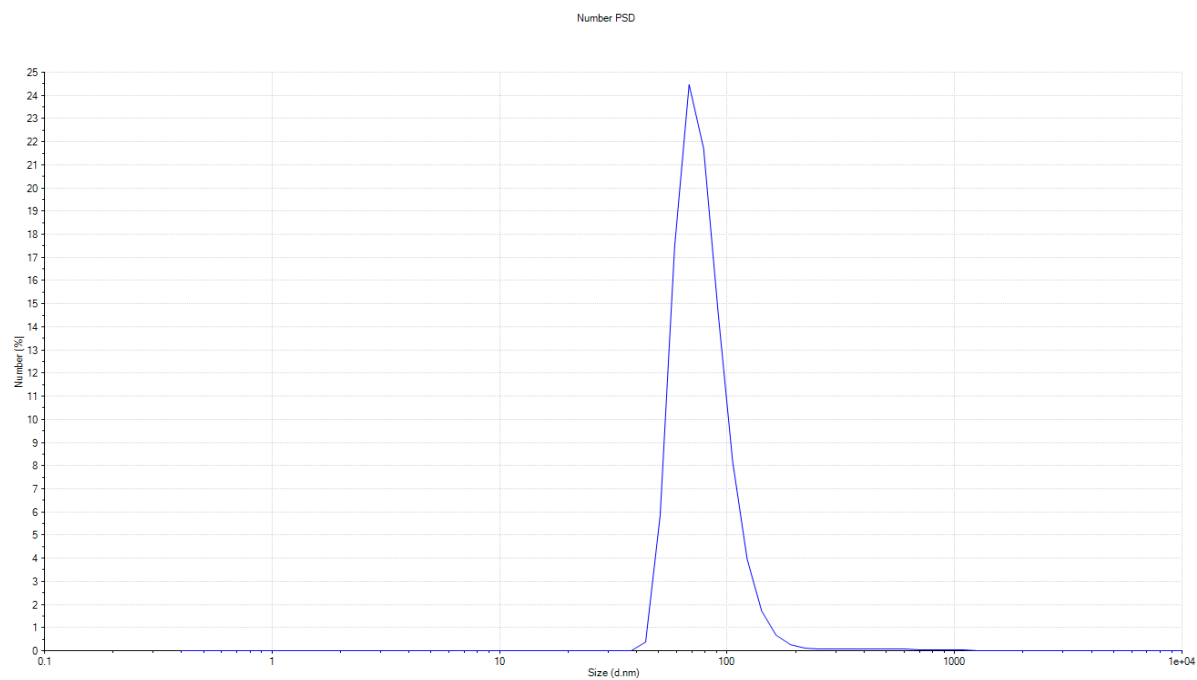


**Figure 23:** Average diameter of mPEG-PLA micelles suspended in ultra-pure DI water determined by dynamic light scattering

#### 6.4 Cell Culture Based Suppression of mPEG-PLA nanoparticles vs Zika Virus

mPEG-PLA nanoparticles were tested against Zika virus to account for any signs of viral suppression from the copolymer alone. Viral suppression techniques include that of a dose dependence assay along with viral titration via plaque assay. Visible plaques were seen which indicated viral suppression.

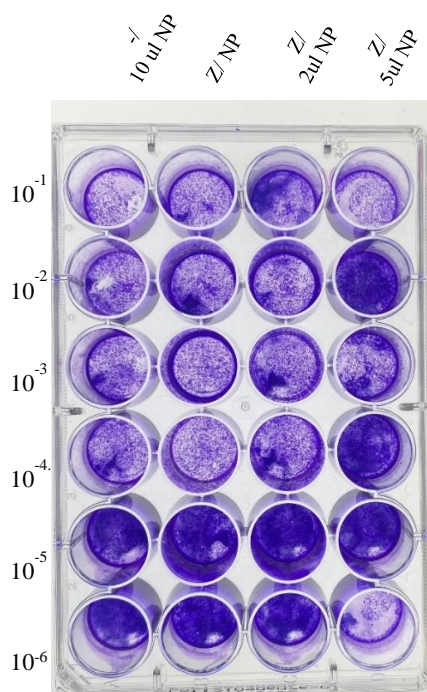


**Figure 24:** Vero cells were plated at  $0.24 \times 10^6$  cells and infected with Zika virus using 10-fold serial dilutions against mPEG-PLA nanoparticles

## CHAPTER 7

### DISCUSSION

Cell culture refers to the process in which cells are grown under controlled conditions. These conditions include temperature, pH, osmotic pressure oxygen and carbon dioxide levels. The growth of cells in laboratories reap myriad benefits as they are used to diagnose infections, test new drugs and play a fundamental role in research. Cell culture suppression techniques such as dose dependence assays and viral titration via plaque assay are well accepted amongst the scientific community as these assays provide fast-generating and reproducible results. With pyridazine derivatives having advantageous physiochemical properties, its integration towards the strategies and development of small molecule inhibitors and drug delivery systems against viruses serves prime importance within research.<sup>44</sup>

Pyridazine derivatives used for the purpose of this research each emphasized a unique structural role as they differed in the attachment of various functional groups (-NH<sub>2</sub>, -Cl and -OCH<sub>3</sub>) which attributed different effects on cell culture. Visualization of the effects was showcased through viral titration via plaque assay which is a direct method for quantification. All derivatives were added to cell plates that contained Vero Cells and 50 µL Zika Virus after calculations of the working concentration of each derivative was done.

Data supports the successful suppression of Zika virus with the use of PY-LP-3 as seen in Figure 15. Success is attributed to the amino functional group. Both PY-LP-6 and PY-LP-12 underwent a vast amount of cell death and were unable to be quantified via plaques. This could have been attributed to the drug itself or the cell line in which we suspected could have been

Dengue which previously had difficulties growing in cell culture. Some limitations of cell culture suppression techniques include contamination and cell line misidentification.

It was necessary to first create a biocompatible polymer that could be shaped into a drug carrier before synthesizing the pH-dependent micelles. mPEG-PLA, an AB, diblock polymer, was created using a previously described procedure. The mPEG or polyethylene glycol that makes up the A monomer was joined to the polylactide that makes up the B monomer to create the AB diblock to create the finished polymer. The polymer underwent characterization after being synthesized to assure proper diblock formation. The complete AB diblock underwent infrared spectroscopy using FTIR infrared spectroscopy.

In order to verify that the proper polymerization took place, the FTIR peaks and distinctive fingerprint regions were compared to published values. The CH stretching present in the mPEG segments is the cause of the peak at  $2900\text{ cm}^{-1}$ . The presence of esters in the PLA segment is shown by the peak at  $1750\text{ cm}^{-1}$  in the diblock polymer. The ether is stretched in part by peaks at  $1000\text{ cm}^{-1}$  in the fingerprint region. The distinctive FTIR spectra's comparison to literature values allowed the polymer's identity—mPEG-PLA—to be verified.

With polymer successfully synthesized the next step was to pursue the synthesis of the nanoparticles. The nanoparticle, drug delivery system used was a single layer micelle made from a diblock polymer. Diblock, biodegradable micelles made from mPEG-PLA were synthesized and characterized. The peak absorbance on the UV-vis spectra for the micelles was 310 nm while the average diameter was 78.96 nm using dynamic light scattering. Due to the mPEG-PLA, not being loaded with any drug, the core can exhibit weak intermolecular forces making it unstable. This instability can be seen between the 300nm -400nm range where there are several bumps. If the mPEG-PLA micelle was Drug-loaded, the curve between this range

would have been smoother and been slightly blue shifted (around 350nm). The average diameter of the mPEG-PLA was 78.96. When compared to literature, this value is acceptable as the average diameter of mPEG-PLA micelles are between 30nm to 100nm.

Due to shortage of the pyridazine derivatives, empty mPEG-PLA nanoparticles were used in cell culture suppression assays to showcase whether or not the particles themselves showcase suppression. This proved to be true as plaque assay of mPEG-PLA and Zika virus showcased plaques which coincides with suppression.

The results noted lays the foundation for a viable drug delivery system that involves novel antivirals encapsulated by biodegradable micellar nanoparticles that target dengue virus and Zika virus with the ability to suppress these viruses.

## CHAPTER 8

### CONCLUSION AND FUTURE OUTLOOK

The main objectives of this research are to create efficient antivirals, a responsive biodegradable diblock, and nanoparticle drug delivery systems that would make it simple to distribute medications inside the body. The information presented in this thesis research demonstrates that efforts to develop antiviral Pyridazine derivatives and diblock polymers against mosquito-borne viruses have been successful.

Future directives of this research call for core drug-load led mPEG-PLA nanoparticles having a certain pH dissociation range, release time, and functionalization capability. Copolymer micellar nanoparticles enhance antiviral drug delivery by increasing drug solubility by encasing the drug molecule until it reaches the desired spot. The trans-Golgi network would be the intended goal in this scenario. With ongoing characterization that includes use of the Zetasizer, NMR and IR analysis, UV-spectroscopy, and microscopy, it is vital to test and examine viral infection suppression capacities against mPEG-PLA blanks and drug-loaded micelles. Cell culture suppression testing with capsuled and encapsulated should also be of utmost importance.

The lack of approved vaccines, medications and treatment regimens against dengue and Zika virus calls for the critical need of antivirals. The possibilities of the biocompatible coblock drug delivery system are not limited to mPEG-PLA and pyridazine derivatives, but rather a step closer to the discovery of a successful solution towards Flaviviridae viruses.

## REFERENCES

1. Knipe, D.; Howley, P. *Fields Virology*, 6th ed.; Lippincott Williams & Wilkins, 2013.
2. Britannica, The Editors of Encyclopedia. "Dmitry Ivanovsky". *Encyclopedia Britannica*, 16 Jun. 2022, <https://www.britannica.com/biography/Dmitry-Ivanovsky>. d 22 2022
3. Chaitanya KV. Structure and Organization of Virus Genomes. *Genome and Genomics*. 2019 Nov 18:1–30.
4. Gelderblom HR. Structure and Classification of Viruses. In: Baron S, editor. *Medical Microbiology*. <https://www.ncbi.nlm.nih.gov/books/NBK8174/>
5. Avila-Perez, G.; Nogales, A.; Martin, V.; et. al.; Reverse Genetic Approaches for the Generation of Recombinant Zika Virus *Viruses* 2018, 10, 597
7. <http://www.niaid.nih.gov/labsandresources/labs/aboutlabs/lvd/viralpathogenesissection/Pages/default.aspx> Diagram by Ted C. Pierson, NIH National Institute of Allergy and Infectious Diseases.
8. Apte-Sengupta S, Sirohi D, Kuhn RJ. Coupling of replication and assembly in flaviviruses. *Curr Opin Virol*. 2014
9. "Flaviviridae." Centers for Disease Control and Prevention, Centers for Disease Control and Prevention, 23 Mar. 2022, <https://www.cdc.gov/vhf/virus-families/flaviviridae>.
10. "Potential Range of Aedes Aegypti and Aedes Albopictus in the United States, 2017." Centers for Disease Control and Prevention, Centers for Disease Control and Prevention, 11 Mar. 2020, <https://www.cdc.gov/mosquitoes/mosquitocontrol/professionals/range.html>.
11. White MK, Wollebo HS, David Beckham J, Tyler KL, Khalili K. Zika virus: An emergent neuropathological agent. *Ann Neurol*. 2016 Oct;80(4):479-89.
12. Dick, O.; Martin, J.; Montoya, R.; Diego, J.; Zambrano, B.; Dayan, G. Review: The History of Dengue Outbreaks in the Americas *Am. J. Trop. Med. Hyg.* 2012, 87, 584-593.
13. Center for Disease Control & Prevention. "Dengue". <https://www.cdc.gov/dengue/index.html>
14. 7. Center for Disease Control and Prevention. "Zika". <https://www.cdc.gov/zika>
15. Naeem, Z.; Zika-Global Concern *Int J Health Sci.* 2016, 10, 5-7
16. Thomas, S.J. and I.K. Yoon, A review of Dengvaxia: development to deployment. *Human Vaccines & Immunotherapeutics*, 2019. 15(10): p. 2295-2314.
17. Hunsperger, E., et al., Dengue pre-vaccination serology screening for the use of Dengvaxia (R). *Journal of Travel Medicine*, 2019. 26(8).
18. Joob, B. and V. Wiwanitkit, Co-circulation of dengue, chikungunya, and Zika viruses and cross-protection. *Rev Panam Salud Publica*, 2019. 43: p. e75.



19. Rico-Mendoza, A., et al., Co-circulation of dengue, chikungunya, and Zika viruses in Colombia from 2008 to 2018. *Rev Panam Salud Publica*, 2019. 43: p. e49.
20. NCBI Bookshelf. "Immune Defenses" <https://www.ncbi.nlm.nih.gov/books/NBK8423/>.
21. Freestone DS. "The need for new antiviral agents". *Antiviral Res.* 1985 Dec;5(6):307
22. Richman DD, Nathanson N. "Antiviral Therapy". *Viral Pathogenesis.* 2016:271–87
23. Orazio A. Attanasi, Gianfranco Favi, Paolino Filippone, Francesca R. Perrulli and Stefania Santeusano, "A Novel and Convenient Protocol for Synthesis of Pyridazines", *Org. Lett.*, 2009, 11 (2), pp 309–312.
25. Richard Hoogenboom, Brian C. Moore, and Ulrich S. Schubert, "Microwave-Assisted Synthesis of 3,6-Di(pyridin-2-yl)pyridazines: Unexpected Ketone and Aldehyde Cycloadditions", *J. Org. Chem.*, 2006, 71 (13), 4903–4909
26. Han, T.; Zong, Q. S.; Chen, C. F. "Complexation of Triptycene-Based Cylindrical Macrotricyclic Polyether toward Diquaternary Salts: Ion-Controlled Binding and Release of the Guests". *J. Org. Chem.* 2007, 72, 3108–3111
27. Shijun Lin, Zhende Liu, and Youhong Hu, "Microwave-Enhanced Efficient Synthesis of Diversified 3,6-Disubstituted Pyridazines", *J. Comb. Chem.*, 2007, 9 (5), pp 742–744.
28. "Aniline - Major Uses." U.S. National Library of Medicine, National Institutes of Health, <https://webwisser.nlm.nih.gov/substance?substanceId=15&identifier=Aniline&identifierType=name&menuItem=22&catId=24>.
29. Beebe-Dimmer JL, Ruterbusch JJ, Bylsma LC, Gillezeau, et al "Patterns of Bicalutamide Use in Prostate Cancer Treatment: A U.S. Real-World Analysis Using the SEER-Medicare Database." *Adv Ther.* 2018 Sep;35(9):1438-1451.
30. "Chlorobenzene (MCB)." PCC Group, 1 Apr. 2019, <https://lp.pcc.eu/mcb/>.
31. Ohashi N, Sakao Y, Yasuda H, Kato A, Fujigaki Y. Methoxy polyethylene glycol-epoetin beta for anemia with chronic kidney disease. *Int J Nephrol Renovasc Dis.* 2012;5:53-60.
32. Ghasemi, R., Abdollahi, M., Emamgholi Zadeh, E. et al. mPEG-PLA and PLA-PEGPLA nanoparticles as new carriers for delivery of recombinant human Growth Hormone(rhGH). *Sci Rep* 8, 9854 (2018).
33. Kunduru, K.; Basu, A.; Domb, A. *Biodegradable Polymers: Medical Applications EPST.*2016, 1-22.
34. Gong, C.; Wei, X.; Wang, X.; Wang, et al., Biodegradable Self-assembled PEG-PCL-PEG Micelles for Hydrophobic Honokiol Delivery: I. Preparation and Characterization *J. Nanotechnol.* 2010, 21, 215103.

35. Ghasemi R, Abdollahi M, Emamgholi Zadeh E, Khodabakhshi K, Badeli A, Bagheri H, Hosseinkhani S. mPEG-PLA and PLA-PEG-PLA nanoparticles as new carriers for delivery of recombinant human Growth Hormone (rhGH). *Sci Rep.* 2018 Jun 29;8(1):9854
36. Sang-Cheol C, Dae-II Y, Sung-Chul K, Eun-Seok P. 2003. A polymeric micellar carrier for the solubilization of biphenyl dimethyl dicarboxylate. *Arch Pharm Res.* 26(2):173-181
37. Makhlof, A.; Abu-Thabit, N. *Stimuli Responsive Polymeric Nanocarriers for Drug Delivery Applications Advanced Nanocarriers for Therapeutics*, 2nd ed.; Woodhead Publishing, 2019.
38. Jhaveri AM, Torchilin VP. Multifunctional polymeric micelles for delivery of drugs and siRNA. *Front Pharmacol.* 2014 Apr 25;5:77.
39. Jo, M.; Lee, Y.; Park, C.; et. al. Evaluation of the Physicochemical Properties, Pharmacokinetics, and In Vitro Anticancer Effects of Docetaxel and Osthol Encapsulated in Methoxy Poly(ethylene glycol)-b-Poly(caprolactone) Polymeric Micelles *Int. J. Mol. Sci.* 2021, 22, 231.
40. Dong Y, Feng SS. Methoxy poly(ethylene glycol)-poly(lactide) (MPEG-PLA) nanoparticles for controlled delivery of anticancer drugs. *Biomaterials.* 2004 Jun;25(14):2843-9.
41. Ammerman NC, Beier-Sexton M, Azad AF. Growth and maintenance of Vero cell lines. *Curr Protoc Microbiol.* 2008 Nov;
42. "Summary of Using Vero Cells in Biology Studies." Oxford Instruments, <https://andor.oxinst.com/learning/view/article/vero-cells>.
43. "The Role of Vero Cells in the Research of Viral Vaccines." AcceGen Biotech, <https://www.accegen.com/recent-posts/the-role-of-vero-cells-in-the-research-of-viral-vaccines/>.
44. Larsson P, Engqvist H, Biermann J, Werner Rönnerman E, Forssell-Aronsson E, Kovács A, Karlsson P, Helou K, Parris TZ. Optimization of cell viability assays to improve replicability and reproducibility of cancer drug sensitivity screens. *Sci Rep.* 2020 Apr 2;10(1)
45. Salahudeen MS, Nishtala PS. An overview of pharmacodynamic modelling, ligand binding approach and its application in clinical practice. *Saudi Pharm J.* 2017 Feb;25(2):165-175
46. Mendoza EJ, Manguiat K, Wood H, Drebot M. Two Detailed Plaque Assay Protocols for the Quantification of Infectious SARS-CoV-2. *Curr Protoc Microbiol.* 2020 Jun;57(1)